

**PARAMETRIC ROLLING IN REGULAR HEAD WAVES OF THE KRISO CONTAINER SHIP:  
 NUMERICAL AND EXPERIMENTAL INVESTIGATION IN SHALLOW WATER**

**Manases Tello Ruiz<sup>1</sup>**

Ghent University  
 Ghent, Belgium

**Guillaume Delefortrie**

Flanders Hydraulics Research  
 Antwerp, Belgium  
 Ghent University  
 Ghent, Belgium

**Jose Villagomez<sup>2</sup>**

Flanders Hydraulics Research  
 Antwerp, Belgium

**Evert Lataire, Marc Vantorre**

Ghent University  
 Ghent, Belgium

**ABSTRACT**

*The IMO Intact Stability Code considers the parametric rolling phenomenon as one of the stability failure modes because of the larger roll angles attained. This hazardous condition of roll resonance can lead to loss of cargo, passenger discomfort, and even (in the extreme cases) the ship's capsize. Studies as such are mostly conducted considering wave characteristics corresponding to wave lengths around one ship length ( $\lambda \approx L_{PP}$ ) and wave amplitudes varying from moderate to rough values. These wave characteristics, recognised as main contributors to parametric rolling, are frequently encountered in deep water. Waves with lengths of such magnitudes are also met by modern container ships in areas in close proximity to ports, but with less significant wave amplitudes. In such areas, due to the limited water depth and the relatively large draft of the ships, shallow water effects influence the overall ship behaviour as well.*

*Studies dedicated to parametric rolling occurrence in shallow water are scarce in literature. In spite of no accidents being yet reported in such scenarios, its occurrence and methods for its prediction require further attention; this in order to prevent any hazardous conditions. The present work investigates the parametric roll phenomenon numerically and experimentally in shallow water. The study is carried out with the KRISO container ship (KCS) hull. The numerical investigation uses methods available in literature to study the susceptibility and severity of parametric rolling. Their applicability to investigate this phenomenon in shallow water is also discussed. The experimental analysis was carried out at the Towing Tank for Manoeuvres in Confined Water at Flanders Hydraulics Research (in co-operation with Ghent University). Model tests comprised a variation of different forward speeds, wave amplitudes and wave lengths (around one  $L_{PP}$ ). The water*

*depth was fixed to a condition equivalent to a gross under keel clearance (UKC) of 100% of the ship's draft.*

Keywords: Parametric rolling; shallow water.

**INTRODUCTION**

Understanding the ship behaviour at sea, under the effect of different environmental conditions, has always been a major goal of the maritime sector. The knowledge gained can be used to enhance the ship's overall behaviour, hence providing better working conditions for the crew meanwhile ensuring safe operations. Parametric rolling is a critical phenomenon which can induce large roll oscillatory motions in only few cycles[1], thus impairing the overall ship performance, increasing the risks of crew casualties, and in the worst scenario the loss of cargo and damage of the ship [2], [3]. The severe observed conditions boosted research on this topic aiming for a better understanding and to provide solutions in order to avoid such dangerous conditions.

The onset of parametric rolling is mostly observed in the following conditions:

- wave lengths ( $\lambda$ ) and the ship length( $L_{pp}$ ) are of comparable order;
- moderate to large wave amplitudes;
- the wave encounter frequency ( $\omega_E$ ) is approximately twice the roll resonance frequency ( $\omega_\phi$ );
- in head or following seas and
- at reduced ship speeds [4], [5].

In these conditions a significant change of GM is experienced as a result of the constantly changing ship's wetted surface. This is especially the case for ships with larger bow flare and overhanging stern such as container ships. An illustration of such a significantly change in the wetted surface

<sup>1</sup> Contact author: Manases.Ruiz@UGent.be

<sup>2</sup> Contact author: Jose.Villagomez@mow.vlaanderen.be

as the wave propagates along the ship's length is shown in Figure 1.

In finite water depth wave lengths comparable to Panamax container ship lengths ( $\lambda \approx 230\text{m}$ ) are rare but yet present, see e.g. Figure 2 ( $\omega_W < 0.5 \text{ rad/s}$ ). In such areas reduced ship speeds are very common, see Figure 3. These are two of the main requirements for the onset of parametric rolling, implying that such phenomenon can also be present in finite water depths. However, as seen in Figure 2 ( $\omega_W < 0.5 \text{ rad/s}$ ) the required waves have a very low occurrence.

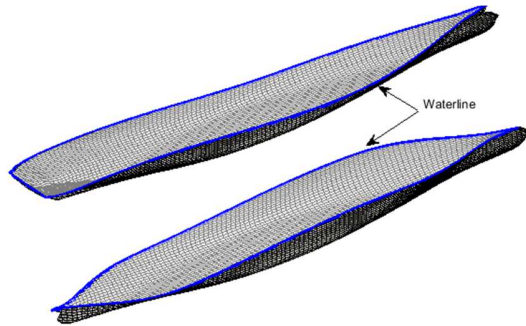


**FIGURE 1.** ILLUSTRATION OF THE CHANGING WETTED SURFACE AS EFFECT OF PASSING WAVE ( $\lambda = L_{pp}$ ).

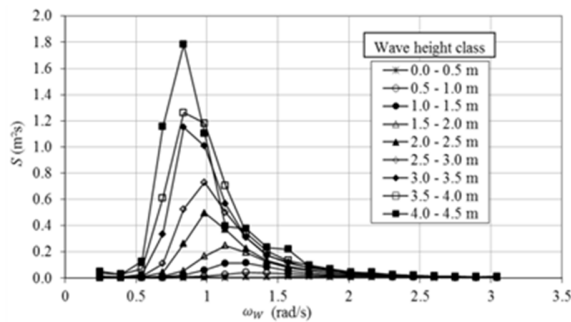


**FIGURE 2.** TYPICAL WAVE SPECTRA IN THE BELGIAN PART OF THE NORTH SEA (RETRIEVED FROM [6]).

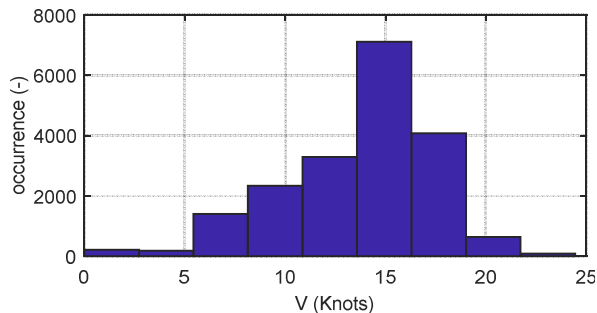


**FIGURE 3.** SAMPLE OF SHIP SPEEDS ATTAINED BY CONTAINER SHIPS IN FINITE WATER DEPTH IN THE ACCESS CHANNELS TO THE MAIN BELGIAN PORTS [7].

Parametric rolling has been addressed in literature in numerous studies, among others see e.g. [4], [8] and [9]. The developed methods vary from simple approximations to more advance methods. For instance, in [2] a one Degree of Freedom (1DoF) “Mathieu-type” oscillator is used, in [5], [7], [11] and [12] a 3DoF coupled heave pitch and roll model has been developed, and in [4] and [13] the analysis is conducted directly using Boundary Element Methods (BEM).

The different methods found in literature can be classified according to susceptibility criteria and severity criteria. Susceptibility criteria can be evaluated by simplified methods. They can already provide information whether or not such phenomenon can occur. The major problem with this approach is that in some cases the onset of parametric rolling cannot be clearly identified; moreover, it cannot be used to determine the final amplitude of the roll motion. In this case severity criteria methods can be used to determine for instance the final attained roll angles; among others, the methods developed in [4], [10] and [13] can be used depending on the desired level of accuracy.

The application of such methods have been extensively investigated in literature with results showing good and fair agreement with experiments (e.g. [10], [4]). Studies as such, to the authors’ best knowledge, are all conducted in deep water. No particular attention has been paid to the finite water depth. This can to some extent be understood because of the limited occurrence of large wave amplitudes in such areas, thus no relevance to study parametric rolling in finite water depth.

Bear in mind that in limited water depths, larger body oscillatory motions are not allowed simply because they may lead to bottom touching. Notice as well that in such scenarios the ship experiences squat effects which induce an additional sinkage and trim. Thus, the already limited under keel clearance (UKC) between the ship’s keel and the sea bottom becomes even more critical, and bottom contact more likely to occur if for moderate ship motions.

Taking into account that in such areas waves of lengths comparable to the ship length are still present, the onset of parametric rolling and the correct estimation of the final roll angles attained becomes then of crucial interest, even if the resulting roll magnitudes are small. The important question to be made is then if the current methods available in literature are still able to predict such phenomenon under the constraint of finite water depth.

The present work investigates the problem of parametric rolling taking into account a finite water depth. Moreover, the study also aims to assess whether current methods are still able to predict its onset and the final roll angle attained. For this purpose experimental and numerical studies will be conducted with a KCS ship. The experimental studies have been conducted at Flanders Hydraulics Research (FHR) with a 1/52.667scale model of the containership. For the numerical analysis, the susceptibility criteria developed by ABS [4] and the severity criteria will be evaluated by using a 3DoF model developed by Neves and Rodríguez[12].

## PARAMETRIC ROLL: MEHTODS

### The ABS Susceptibility Criteria

This method [4] is a simplified approach where the problem of parametric rolling is modelled in 1DoF as:

$$\ddot{\phi} + 2\delta\dot{\phi} + \frac{\rho g \nabla GM(t)}{(I_{xx} + A_{44})} \phi = 0 \quad (1)$$

where  $\delta$  is the linearised damping,  $I_{xx}$  is the transversal mass moment of inertia,  $A_{44}$  is the added moments of inertia in roll and  $GM(t)$  is the changing transversal metacentric height.

The time dependency of  $GM$  is expressed harmonically, see Eq. 2, taking into account only the first order approximation.

$$GM(t) = GM_m + GM_a(t) \cos(\omega_E t) \quad (2)$$

In Eq. (2) the subscripts “m” and “a” refer to the mean and the amplitude of the oscillatory characteristics of the first order fitting of  $GM$ . Eq. (1) and (2) are approximations which help to express the roll motion problem in the form of the Mathieu equation as:

$$\frac{dx^2}{d\tau^2} + (p + q \cos(\tau))x = 0 \quad (3)$$

The solution of Eq.(3) can be classified as bounded and unbounded as mentioned in [4]. The unbounded solutions correspond to the instability zones where parametric roll occur.

All possible combinations of the parameters  $p$  and  $q$  can be displayed in a figure commonly known as the Ince-Strutt diagram. Thus in order to determine whether the ship is prone to parametric rolling phenomenon it is only required to estimate the  $p$  and  $q$  parameters and plot them in the Ince-Strutt diagram.

The major problem with this method is that in the case where parametric rolling is identified, the solution predicts unbounded roll angles. The latter is, however, not realistic because even when parametric rolling occurs, the nonlinearities in the damping and restoring terms will eventually dissipate more energy than the gained one. Thus a new dynamic equilibrium will be found. This is not predicted by the solutions of the Mathieu-type oscillator. To identify this magnitude in [4] an additional simplified method is proposed but because of its simple approximations it will not be used.

### The Severity Criteria by a 3rdorder Coupled Model

To evaluate the severity of the parametric rolling problem the method proposed in [12], [14] will be used. In this method a 3DoF coupled heave ( $z$ ), roll( $\phi$ ) and pitch ( $\theta$ ) model based on the Taylor series expansion up to the 3<sup>rd</sup> order is proposed. The method approximates all forces and moments depending on the relative ship position with respect to the incident wave. The general equation describing all modes of motions can be expressed as:

$$(\mathbf{M} + \mathbf{A})\dot{\mathbf{s}} + \mathbf{B}(\dot{\mathbf{s}})\dot{\mathbf{s}} + \mathbf{c}_r(\mathbf{s}, \zeta) = \mathbf{c}_{Ext}(\zeta, \dot{\zeta}, \ddot{\zeta}) \quad (4)$$

where  $\mathbf{M}$  is the rigid body inertia of the ship,  $\mathbf{A}$  is the hydrodynamic (added) inertia,  $\mathbf{B}$  is the nonlinear hydrodynamic damping,  $\mathbf{c}_r$  is the nonlinear restoring moment,  $\mathbf{c}_{Ext}$  is the external wave excitation forces,  $\mathbf{s}$  is the state variable, and the upper dots indicate time derivatives.

In Eq. (4) the matrices  $\mathbf{A}$ ,  $\mathbf{B}$ , and  $\mathbf{s}$  are given as:

$$\mathbf{A} = \begin{bmatrix} Z_z & 0 & Z_{\dot{\theta}} \\ 0 & K_{\dot{\phi}} & 0 \\ M_{\dot{z}} & 0 & M_{\dot{\theta}} \end{bmatrix}; \mathbf{B} = \begin{bmatrix} Z_z & 0 & Z_{\dot{\theta}} \\ 0 & K(\dot{\phi}, |\dot{\phi}|) & 0 \\ M_{\dot{z}} & 0 & M_{\dot{\theta}} \end{bmatrix}; \mathbf{s} = \begin{bmatrix} z \\ \phi \\ \theta \end{bmatrix} \quad (5)$$

where the roll damping term  $K(\dot{\phi}, |\dot{\phi}|)$  is decomposed in a linear  $b_{\dot{\phi}}$  (skin friction dependent) and a nonlinear  $b_{\dot{\phi}}|\dot{\phi}|$  (viscous dependent) component.

The major development of the present method is with respect to the restoring moment  $\mathbf{c}_r$ . This term depends on the relative motions between the ship hull and the wave elevation  $\zeta$  and it is subdivided in five terms as shown in Eq. (6).

$$\mathbf{c}_r = \mathbf{c}_r^{(1)} + \mathbf{c}_{r(m)}^{(2)} + \mathbf{c}_{r(w)}^{(2)} + \mathbf{c}_{r(m)}^{(3)} + \mathbf{c}_{r(w)}^{(3)} \quad (6)$$

The five terms in Eq. (6) can be grouped by their order of the Taylor series expansion, first, second, and third, or by the action they depend upon, hydrostatic  $r$ , ship motions  $r(m)$ , or wave type ( $w$ ).

Regarding the external forces  $\mathbf{c}_{Ext}$  in Eq. (4), as mentioned in [12], they are computed as the sum of the Froude-Krylov and diffraction problem computed over the mean wetted surface.

The results obtained from the analysis of the current method can be described with more detail in numerical maps as proposed in [15] and [16]. These maps delimit the boundaries of instability and also contain the information of the attained roll amplitude during the event of parametric rolling.

## EXPERIMENTAL PROGRAM

### The Towing Tank

The experimental program was conducted in the Towing Tank for Manoeuvres in Confined Water at Flanders Hydraulics Research (in co-operation with Ghent University). The towing tank main dimensions are a total length of 87.5 m, a width of 7.0 m and a maximum water depth of 0.5 m. It is implemented with a carriage mechanism and wave maker.

The carriage mechanism is composed of two main carriages, a main longitudinal one and a secondary transversal one, in addition to a yawing table. The wave maker is located at the opposite side of the harbour and can be used to generate unidirectional regular and irregular waves. More detailed information on the towing tank can be found in [17].

### The Model Test Setup

The ship model is mounted to the carriage mechanism by means of a beam frame which is attached to the ship by a pitch and roll mechanism which connect the ship to the carriage via a set of two vertical guidance systems. See Figure 4a for a better illustration. The setup allows semi-captive tests with the model

free to move vertically and to rotate in roll (along the  $x$ -axis) and pitch (along the  $y$ -axis). These modes of motion can be restrained independently from each other, thus allowing all possible combinations.

During tests time records of two composed strain gauges LC1 and LC2, and four potentiometers P1 to P4 are registered. From these measurements forces (in surge and sway), moments (in yaw) and motions (heave, roll and pitch) can be derived. Wave profiles along the tank (at a fixed position) and at a constant distance from the ship (as seen by the ship) have also been recorded during tests. For this purpose resistant type (for the fixed ones) and a laser beam type (for the moving one) wave gauges have been used. The position of the latter (WG1) is displayed in Figure 4. More details on the resistive type wave gauges has been omitted hereafter for the sake of brevity as they were only used to verify the wave profiles along the tank.

Note that to describe the ship position, orientation and the measurements all coordinate systems are North East Down (NED) oriented. See for instance the body fixed axes system  $Oxyz$  displayed in Figure 4b.

### Test Matrix

The ship speeds, the wave lengths, and their respective combinations have been selected to meet the main requirement for the onset of parametric rolling. Note as well that these parameters do correspond to scenarios found, less frequent but present, in the Belgian part of the North Sea (see Figure 2 and Figure 3). The respective values and pairs are shown in Table 2.

The numerical evaluation of parametric roll is sensitive to the accurate estimation of the total roll damping. For this purpose, free roll decay tests have been conducted at two different speeds and two different initial roll angles ( $\phi_i$ ). The chosen parameters are presented in Table 3. Figure 5 illustrates the two different test types conducted in the present study.

### Ship Model

The tests have been carried out with a scale model of the KRISO container ship (KCS). The main characteristics are given at full scale in Table 1.

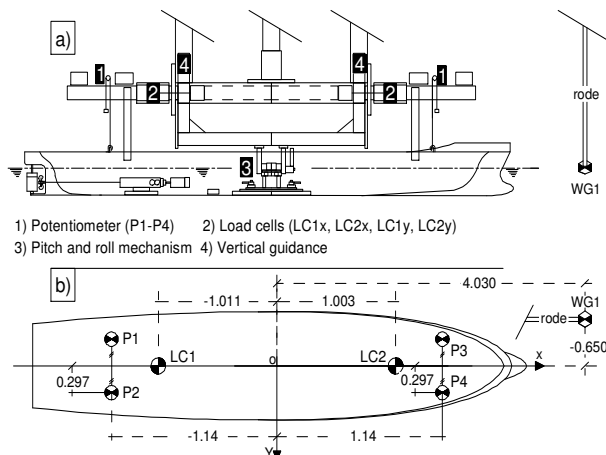


**FIGURE 4.** BEAM FRAME AND INSTRUMENTATION ARRANGEMENT DURING TESTS

**TABLE 1.** THE KCS MAIN CHARACTERISTICS.

Item	Description	Value	Units
$LOA$	Length over all	232.50	( $m$ )
$Lpp$	Length between perpendiculars	230.0	( $m$ )
$B$	Breadth	32.20	( $m$ )
$D$	Depth of ship	23.70	( $m$ )
$T_m$	Draft, amidships	10.80	( $m$ )
$C_b$	Block coefficient	0.65	(-)
$m$	Ship's mass	52045.6	( $ton$ )
GM	Transversal metacentric height	0.535	( $m$ )
$R_{xx}$	Longitudinal radius of inertia	12.11	( $m$ )
$R_{yy}$	Transverse radius of inertia	56.67	( $m$ )
$R_{zz}$	Vertical radius of inertia	57.41	( $m$ )
$x_G$	Longitudinal position centre of gravity	-3.69	( $m$ )
$y_G$	Transverse position centre of gravity	0.00	( $m$ )
$z_G$	Vertical position centre of gravity	-3.58	( $m$ )
	Model scale:	52.667	(-)

**TABLE 2.** FULL SCALE SHIP SPEEDS, WAVE LENGTHS AND AMPLITUDES USED FOR PARAMETRIC ROLL TESTS.

$V$ (kn)	$Fr$ (-)	$\lambda/Lpp$ (-)	$\zeta_A$ (m)	$\mu$ (deg)
0.00	0.000	0.97, 1.00, 1.02	0.79, 1.05, 1.58	180
3.2	0.034	1.10	0.79, 1.05, 1.58	180

**TABLE 3.** MAIN PARAMETERS FOR THE FREE ROLL DECAY TESTS.

$V$ (kn)	$Fr$ (-)	$\phi_i$ (deg)
0.00	0.000	6, 9
3.2	0.034	6, 9

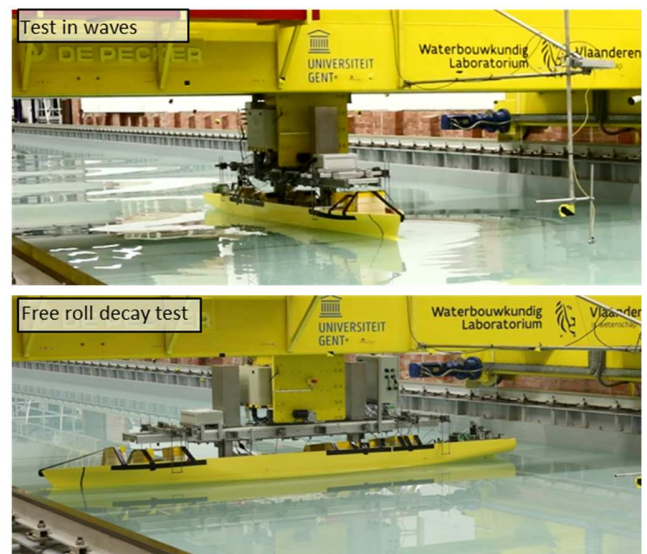


**FIGURE 5.** SAMPLE PHOTOS TAKEN DURING TEST IN WAVES (ABOVE) AND FREE ROLL DECAY TEST (BELOW).

## TEST RESULTS AND DISCUSSIONS

### Free Roll Decay Tests

To identify the linear ( $b_{\dot{\phi}}$ ) and nonlinear ( $b_{\dot{\phi}|\dot{\phi}|}$ ) terms, free roll decay tests have been modelled in 1DoF in the time domain. The contribution of the potential flow has been accounted for by means of a constant added mass ( $A_{44}^{\infty}$ ) and the impulse response function ( $h_{44}$ ), see Eq. (7).

$$(I_{xx} + A_{44}^{\infty})\ddot{\phi} + b_{\dot{\phi}}\dot{\phi} + b_{\dot{\phi}|\dot{\phi}|}|\dot{\phi}|\dot{\phi} + \int h_{44}(\tau - t)\dot{\phi}(t)dt + f(\phi) = 0 \quad (7)$$

$A_{44}^{\infty}$  and  $h_{44}$  have been obtained from numerical simulations carried out with HydroStar.  $A_{44}^{\infty}$  was found to be around 13.2% of  $I_{xx}$  and the impulse response function is displayed in Figure 6. In Eq. (7) the restoring function  $f(\phi)$  is an odd polynomial of fifteenth-order, see Eq.(8), obtained by fitting the GZ restoring curve. A higher order fit was used to allow numerical predictions where larger roll angles are attained. The respective coefficients are given in Table 4.

$$f(\phi) = a\phi + b\phi^3 + c\phi^5 + d\phi^7 + e\phi^9 + f\phi^{11} + g\phi^{13} + h\phi^{15} \quad (8)$$

To obtain the damping coefficients  $b_{\dot{\phi}}$  and  $b_{\dot{\phi}|\dot{\phi}|}$  the method used is similar as the one described in [18]. Instead of solving the integro-differential equation and then applying a nonlinear least square fit, first a nonlinear spline fitting of the roll motion has been obtained, then the first and second order derivatives are obtained. These magnitudes are introduced in Eq. (7), all terms except the ones including the second order derivative are moved to the right hand side, and finally the damping terms  $b_{\dot{\phi}}$  and  $b_{\dot{\phi}|\dot{\phi}|}$  are found by solving the overdetermined system via a simpler least square. More details with respect to the present method can also be found in [19].

An example of the fitted results obtained at zero forward speed is presented in Figure 7. All results for the linear and nonlinear damping coefficients are given in Table 5.

It can be seen from Table 5 that both coefficients are dependent of the ship speed. Each of these values will be used further in the study.

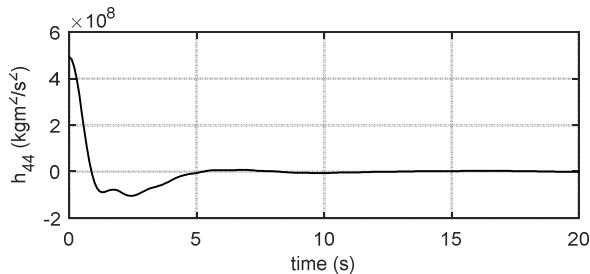


FIGURE 6. ROLL IMPULSE RESPONSE FUNCTION  $h_{44}$ .

TABLE 4. COEFFICIENTS OF THE FUNCTION  $f(\phi)$ .

Coefficients in kNm for $\phi$ in rad					
$a$	2.83E+05	$c$	-2.52E+07	$e$	-2.68E+09
$b$	1.31E+06	$d$	4.11E+08	$f$	8.04E+09
		$g$	-1.15E+10	$h$	6.34E+09

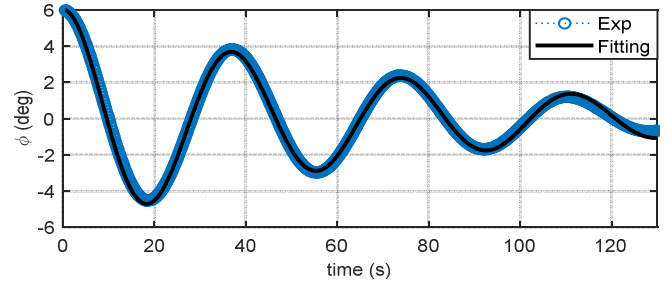


FIGURE 7. FREE ROLL DECAY TESTS AND FITTED NUMERICAL RESULTS AT ZERO FORWARD SPEED.

TABLE 5. LINEAR AND NONLINEAR DAMPING COEFFICIENTS FOR ALL TEST CASES.

$Fr$ (-)	$\phi_i$ (deg)	$b_{\dot{\phi}}$ (kgm <sup>2</sup> /s)	$b_{\dot{\phi} \dot{\phi} }$ (kgm <sup>2</sup> )	Tol (-)
0	6	2.379E+08	2.378E+06	E-12
0.034	6	2.434E+08	2.499E+06	E-12

### Parametric Rolling Tests

The post-processing of all tests in waves has been conducted in order to investigate whether there is an indication of parametric rolling phenomenon. For this purpose, tests where the roll angle increases have been classified as Yes, and test where no change in the initial roll angle is observed has been classified as No. The results from the analysis for all tests are shown in Table 6.

The results in Table 6 indicate that from the twelve tests nine of them (non-shaded) seem to be under the effect of parametric rolling phenomenon. The other three tests, where no effect is observed (shaded), are: two are zero forward speed and tested with the lower wave amplitudes and, one at non-zero forward speed and with the smaller wave amplitude.

TABLE 6. ANALYSIS OF PARAMETRIC ROLLING OCCURRENCE DURING MODEL TESTS.

CASE	$\zeta_A$ (m)	$\lambda/Lpp$ (-)	$Fr$ (-)	Parametric rolling
C01	0.79	0.97	0.0	No
C02	1.05	0.97	0.0	Yes
C03	1.58	0.97	0.0	Yes
C04	0.79	1.00	0.0	No
C05	1.05	1.00	0.0	Yes
C06	1.58	1.00	0.0	Yes
C07	0.79	1.02	0.0	Yes
C08	1.05	1.02	0.0	Yes
C09	1.58	1.02	0.0	Yes
C10	0.79	1.10	0.034	No
C11	1.05	1.10	0.034	Yes
C12	1.58	1.10	0.034	Yes

**NUMERICAL LIMITS OF STABILITY**  
**The Susceptibility of the Parametric Rolling Phenomenon**

For the susceptibility analysis, first the equivalent linear non-dimensional damping term ( $\delta/\omega_\phi$ ) is required. This value has been obtained by applying the energy loss method [20] and the linear and nonlinear damping values obtained from the free roll decay tests. The respective values for the zero and non-zero forward speed are presented in Table 7.

**TABLE 7. NON-DIMENSIONAL LINEARISED DAMPING.**

$Fr$ (-)	$\omega_\phi$ (rad/s)	$\phi_A$ (deg)	$\delta/\omega_\phi$ (-)
0	0.168	6	0.072
0.034	0.168	6	0.073

The change of  $GM(t)$  over time, and the corresponding amplitude  $GM_a$  and mean  $GM_m$  values have been evaluated by using a panel discretisation of the hull as shown in Figure 1. An example of these calculations are shown in Figure 8 for the case C03 (see Table 6).

From all tests the respective  $p$  and  $q$  values are obtained and plotted in the Ince-Strutt diagram in Figure 9. It can be seen from this figure that all tests are subjected to parametric rolling phenomenon. Notice that tests showing a clear influence (farther from the instability boundaries) of this problem are the ones where the wave amplitude is larger.

Comparing the results with experiments, see Table 8, one can observe that the method present three false positive cases, C01, C04, and C10, which correspond to those tests laying in close proximity to the instability boundaries. In literature, similar results are found for such cases and the discrepancies are mainly presumed due to nonlinearities in the roll motion equation. This will be further studied with a more advanced method to check if it can better capture the problem.

In spite of the disagreement with some of the experimental results one can state, however, that the ABS method is able to predict conservatively the occurrence of parametric rolling.

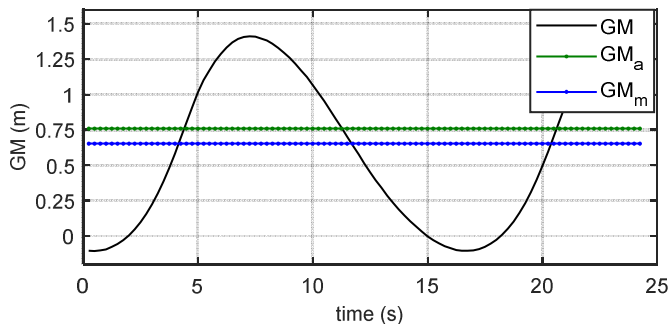


**FIGURE 8. THE CHANGING  $GM(t)$  OVERTIME, THE AMPLITUDE  $GM_a$  AND MEAN  $GM_m$  VALUES AS THE WAVE PROPAGATES ALONG THE SHIP FOR TEST CASE C03.**

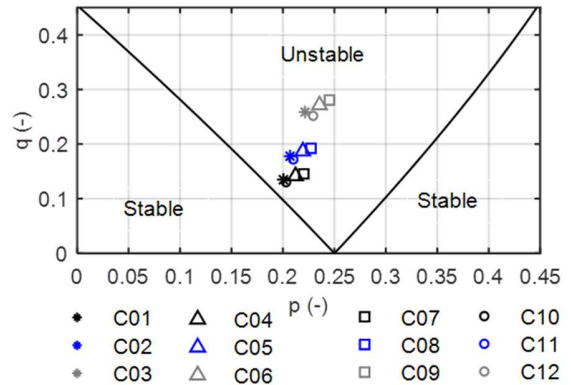


**FIGURE 9.  $p$  AND  $q$  VALUES FOR ALL TEST DISPLAYED IN THE INCE-STURTT DIAGRAM.**

**TABLE 8. PREDICTION ASSESSMENT OF PARAMETRIC ROLLING (PR) OCCURENCE.**

CASE	Test	ABS	Agreement
C01	No	Yes	✗
C02	Yes	Yes	✓
C03	Yes	Yes	✓
C04	No	Yes	✗
C05	Yes	Yes	✓
C06	Yes	Yes	✓
C07	Yes	Yes	✓
C08	Yes	Yes	✓
C09	Yes	Yes	✓
C10	No	Yes	✗
C11	Yes	Yes	✓
C12	Yes	Yes	✓

**The Severity of the Parametric Rolling Phenomenon**

For the numerical study of severity, the results are presented in a form of instability maps (see e.g. Figure 10). To obtain these maps, time-domain simulations are performed in order to detect the roll angle amplification which is defined at the condition where the ship reaches a new dynamic steady state with a constant roll amplitude. These simulations are computed in each point of a grid which corresponds to different combinations of wave amplitude and wave frequency for the specified ship's forward velocity.

For the present study the simulation time was set to 25min for all the test cases, the wave amplitude varied up to 3.5m, and the range of wave frequency was chosen from 0.25 to 0.75 rad/s. Note that in the maps (see Figure 10 and Figure 11) the results are plotted as a function of the wave amplitude and the encounter frequency, the latter being non-dimensionalised by the ship's roll natural frequency (0.1875 rad/s).

From the analysis of all tests the resulting instability maps for zero speed and 3.2 knots are presented in Figure 10 and Figure 11, respectively. In Figure 10 and Figure 11 the test cases are also displayed to allow better comparison with the numerical results.

From the zero speed case (Figure 10) it can be seen that the 3DoF model predicts four cases (C01, C02, C04 and C07) where parametric rolling does not occur and, for the case at 3.2knots (Figure 11) only one case (C10) is free of this phenomenon. Comparing the numerical results with the experiments, see Table 9, the 3DoF model appears to miss-predict the onset of parametric rolling only for two cases, C02 and C07.

The numerical results seem to agree better for the non-zero forward speed cases where all tests have been predicted correctly. To have a better idea of the numerical simulation the time series for the cases C10 and C11 are shown in Figure 12 and Figure 13, respectively, as an example. In Figure 12 no amplification of the roll motion is observed while in Figure 13 the onset of parametric rolling phenomenon is fairly predicted. It is important to mention that the experimental assessment of roll amplification was limited to 5 deg to prevent capsizing or shifting ballast, hence the final roll angle amplification could not be validated. However, the simulations show (see e.g. Figure 13) acceptable agreement in the initial cycles of the measured roll angle where the parametric rolling phenomenon occurs.

At zero forward speed the two cases where false negatives are obtained (C02 and C07) are close to the boundary of instability. It is known that this boundary delimited by the present 3DoF model is strongly affected by the initial conditions of the simulation due the non-linear approach; what is more, this method loses accuracy as the variation of the flare is more significant near the waterline. This could explain the discrepancies encountered. However, these remarks do not clear the question why major discrepancies are obtained at zero forward speed. To have a more clear idea of what happens in these particular cases a more detailed analysis is required which can be conducted in further studies. The set of test C02, C04, C05, C07 and C10 could be used for this purpose.

In spite of the discrepancies encountered it can be stated that the 3DoF model is able to predict fairly well the onset of parametric rolling in shallow water, see Table 9. However, a major concern is with respect to the model prediction for the cases C02 and C07, where false negatives are obtained. These are cases which require further attention to identify if the miss prediction is due to the method itself or uncertainties in the experiments, e.g. in the measurement of the GM.

Notice that the method for the cases where parametric rolling has been predicted, the maximum roll angles estimated are around 8 deg., see Table 9. Although this value is less severe as observed in open seas (roll angles up to 40 deg are reported [2]), 8 deg roll motion would lead to dangerous conditions, e.g. shifting of cargo. Moreover, considering the limited depth the drastically reduction of the available UKC deserved attention, as this could lead to bottom touching when a lower UKC is considered and should be further investigated.

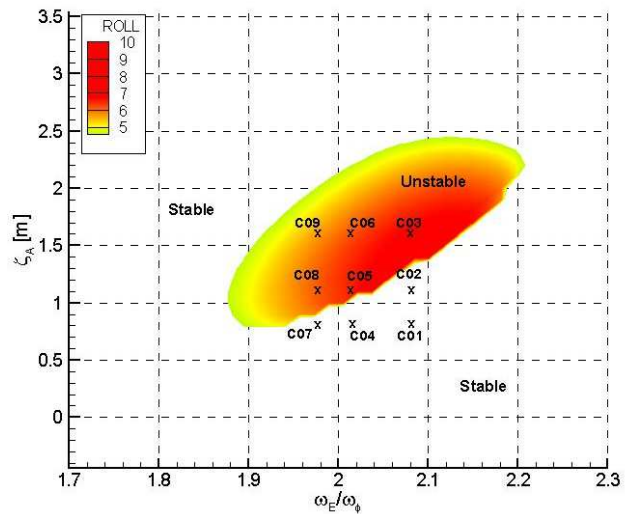


FIGURE 10. ROLL INSTABILITY REGION AT ZERO FORWARD SPEED.

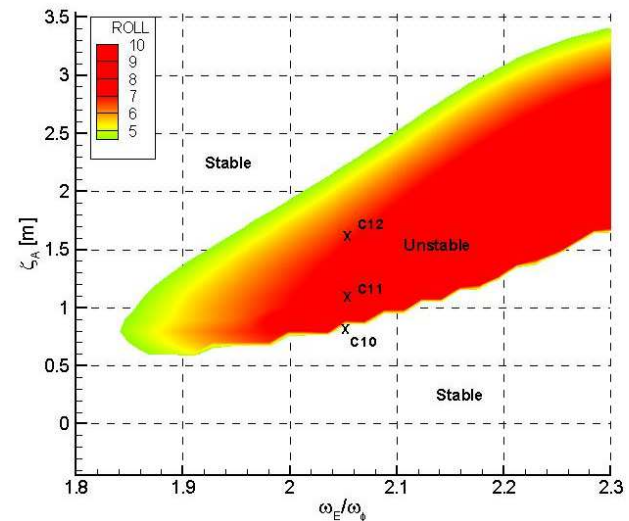
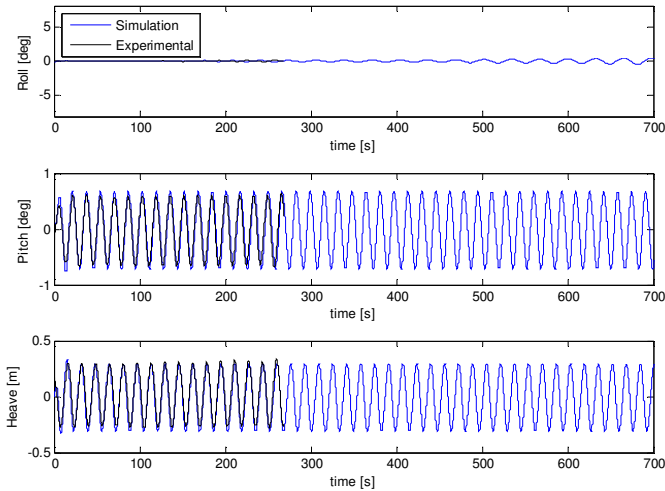


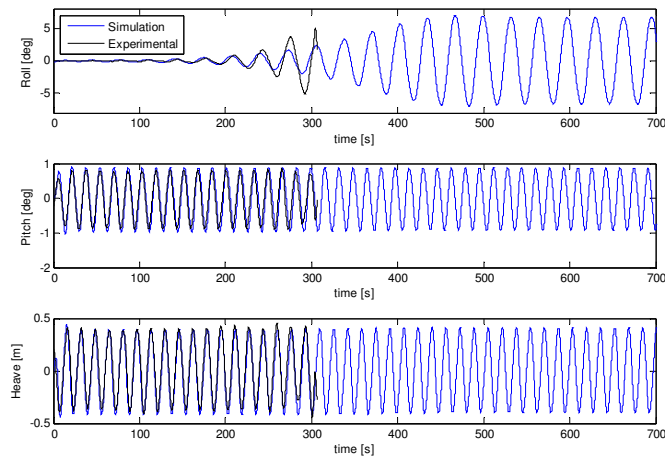
FIGURE 11. ROLL INSTABILITY REGION AT 3.2 KNOTS.

TABLE 9. PREDICTION ASSESSMENT OF PARAMETRIC ROLLING (PR) OCCURRENCE.

CASE	Test	3DoF Model	Agreement	$\phi_a$ , (deg)
C01	No	No	✓	-
C02	Yes	No	✗	-
C03	Yes	Yes	✓	7.01
C04	No	No	✓	-
C05	Yes	Yes	✓	6.25
C06	Yes	Yes	✓	6.15
C07	Yes	No	✗	-
C08	Yes	Yes	✓	6.32
C09	Yes	Yes	✓	5.63
C10	No	No	✓	-
C11	Yes	Yes	✓	7.66
C12	Yes	Yes	✓	6.77



**FIGURE 12.** TIME SERIES FOR THE NON ZERO FORWARD SPEED CASE C10.



**FIGURE 13.** TIME SERIES FOR THE NON ZERO FORWARD SPEED CASE C11.

## CONCLUSIONS

The present study investigates whether a Panamax container ship (the KCS) navigating in shallow water can be subjected to the parametric rolling phenomenon and, if such is the case, evaluates the applicability of two well-known approaches to predict its onset. The methods used are the 1DoF roll model proposed in Shin et al. [4] and the 3DoF coupled heave, roll and pitch model developed by Neves and Rodríguez [12], [14].

From the experimental evaluation it has been observed that in shallow water conditions parametric rolling may also occur. This could be attributed to the low GM (0.530m) for this ship which could be claimed as very low; however, it should be stressed that this value still satisfies the minimum GM required. Hence, being representative for ships approaching or leaving a port. The latter raises the question whether this problem has

been overlooked by researchers. It is obvious that in shallow water conditions the occurrence of large wave amplitudes is very limited, hence the expected roll angles attained are small and not important when contrasted to deep water cases. One must consider, however, that at limited water depth even small roll angles attained may lead to grounding, hence the relevance to consider this problem in shallow water as well.

With respect to the prediction of the onset of parametric rolling by the first method, the results from this analysis seem to be conservative as all tests evaluated fall inside the unstable region. Hence, indicating a possibility to suffer from parametric rolling phenomenon. From the analysis using the second method, the predictions presented a good agreement detecting the parametric rolling occurrence, only two out of twelve simulations did not match the experiments.

Some false positives and negatives have been obtained with both methods, especially for tests located close to the boundary of instability. Further research is required to determine whether these discrepancies are attributed to the initial conditions, the uncertainty of the measurements or other causes.

In spite of the discrepancies encountered for some cases from the analysis of both methods, one can state that both can be used to predict the onset of the parametric rolling phenomenon although attention is needed when the results are close to the instability boundaries.

Further investigation is also required at lower UKCs and higher speeds (e.g. 14 to 16 knots are more common) in order to assess the influence of squat effects on the onset of parametric rolling and the final roll angles attained during such events.

## REFERENCES

- [1] M. A. S. Neves, J. A. Merino, and C. A. Rodríguez, "A nonlinear model of parametric rolling stabilization by anti-roll tanks," *Ocean Eng.*, vol. 36, no. 14, pp. 1048–1059, 2009.
- [2] W. N. France, M. Levadou, T. W. Treacle, J. Randolph Paulling, R. Keith Michel, and C. Moore, "An investigation of head-sea parametric rolling and its influence on container lashing systems," *SNAME Annu. Meet.*, pp. 1–19, 2001.
- [3] S. M. Carmel and Trb, "Study of parametric rolling event on a Panamax container vessel," *Int. Waterw. Ports, Shipp.*, vol. 5, no. 1963, pp. 56–63, 2006.
- [4] Y. Shin, V. Belenky, and J. Paulling, "Criteria for parametric roll of large container ships in longitudinal seas. Discussion," *Am. Bur. Shipp. Tech. Pap.*, pp. 117–147, 2004.
- [5] N. Umeda, M. Sakai, N. Fujita, A. Morimoto, D. Terada, and A. Matsuda, "Numerical prediction of parametric roll in oblique waves," *Ocean Eng.*, vol. 120, pp. 212–219, 2016.
- [6] M. Vantorre and J. Journée, "Validation of the strip theory code SEAWAY by model tests in very shallow water," *Flanders Hydraul. Res. Numer. Model.*



- Colloquium*, 2003.
- [7] M. Tello Ruiz, “Manoeuvring model of a container vessel in coastal waves,” *PhD thesis, Ghent University, Ghent Belgium*, 2018.
- [8] M. A. S. Neves, J. E. M. Vivanco, and C. A. Rodríguez, “Nonlinear dynamics on parametric rolling of ships in head seas,” in *10th International Conference on Stability of Ships and Ocean Vehicles*, 2009, pp 509-520.
- [9] K. J. Spyrou, I. Tigkas, G. Scanferla, N. Pallikaropoulos, and N. Themelis, “Prediction potential of the parametric rolling behaviour of a post-panamax containership,” *Ocean Eng.*, vol. 35, no. 11–12, pp. 1235–1244, 2008.
- [10] C. Holden, R. Galeazzi, C. Rodríguez, T. Perez, T. I. Fossen, M. Blanke, and M. De Almeida Santos Neves, “Nonlinear container ship model for the study of parametric roll resonance,” *Model. Identif. Control*, vol. 28, no. 4, pp. 87–103, 2007.
- [11] M. A. S. Neves, “On the excitation of combination modes associated with parametric resonance in waves,” in *Proc. of the 6th International Ship Stability Workshop*, 2002.
- [12] M. A. S. Neves and C. A. Rodríguez, “A coupled third order model of roll parametric resonance,” *Marit. Transp. Explor. Ocean Coast. Resour.*, pp. 243–253., 2005.
- [13] T. Kim and Y. Kim, “Multi-level approach for parametric roll analysis,” *Int. J. Nav. Archit. Ocean Eng.*, vol. 3, no. 1, pp. 53–64, 2011.
- [14] M. A. S. Neves and C. A. Rodríguez, “A non-linear mathematical model of higher order for strong parametric resonance of the roll motion of ships in waves,” *Mar. Syst. Ocean Technol. – J. SOBENA*, vol. 1, no. 2, pp. 69–81, 2005.
- [15] M. A. S. Neves and C. A. Rodríguez, “An investigation on roll parametric resonance in regular waves,” *Int. Shipbuild. Prog.*, vol. 54, no. 4, pp. 207–2025, 2007.
- [16] M. A. S. Neves and C. A. Rodríguez, “Influence of non-linearities on the limits of stability of ships rolling in head seas,” *Ocean Eng.*, vol. 34, no. 11–12, pp. 1618–1630, 2007.
- [17] G. Delefortrie, S. Geerts, and M. Vantorre, “The towing tank for manoeuvres in shallow water,” in *Proceedings of the 4th International Conference on Ship Manoeuvring in Shallow and Confined Water*, 2016, pp. 226–235.
- [18] J. M. Varah, “A Spline Least Squares Method for Numerical Parameter Estimation in Differential Equations,” *SIAM J. Sci. Stat. Comput.*, vol. 3, no. 1, pp. 28–46, 1982.
- [19] C. Chen, M. Tello Ruiz, G. Delefortrie, E. Lataire, M. Tianlong, and M. Vantorre, “Parameter estimation for a ship ’ s roll response model in shallow water using an intelligent machine learning method,” in *MASHCON 2019: International conference on ship manoeuvring in shallow and confined water*, 2019.
- [20] F. Tasai, “Equation of ship roll motion,” *Re. Inst. Appl. Mech. Kushu Univ. (In Japanese)*, vol. Rep. No. 2, 1965.